

Evaluation of Yellow Rust Reactions in some Bread and Durum Wheat Varieties by Using Spectral Band Regions

Bazı Ekmeklik ve Makarnalık Buğday Çeşitlerinde Spektral Bant Bölgeleri Kullanılarak Sarı Pas Hastalık Reaksiyonlarının Değerlendirilmesi

Metin Aydoğdu^{1*}, Kadir Akan²

¹ Soil, Fertilizer and Water Resources Central Research Institute 06172, Ankara/Türkiye.

² Kırşehir Ahi Evran University, Agriculture Faculty, Plant Protection Department, 40200, Kırşehir/Türkiye.

ORIGINAL PAPER

*Corresponding author:

Metin Aydoğdu
metin.aydogdu@tarimorman.gov.tr

doi: 10.48123/rsgis.1198224

Article history:

Received: 02.11.2022

Accepted: 02.07.2023

Published: 28.09.2023

Abstract

Yellow rust (caused by *Puccinia striiformis* f. sp. *tritici*) is an important fungal disease affecting wheat production and quality. The purpose of this study was to identify the spectral band regions that influence how the disease changes throughout the year by determining how the plant responds to yellow rust when it is applied to test materials at various doses (0%, 25%, 50%, and 100%). Eser, Bayraktar 2000 and Demir 2000 varieties showed high correlation in the early-mid period of the study for bread varieties, while Kenanbey variety exhibited high correlation in the mid-late period. Effective band region for all bread types are The Red+Red Edge+ Near Infrared (NIR) range and NIR range of the Kenanbey variety both showed an increase (+) in disease severity values. Eminbey and Çeşit-1252 varieties for durum varieties displayed high correlation in the early period, followed by Mirzabey 2000 variety in the early to medium period and Kızıltan-91 variety the mid to late period. Kızıltan 91 variety in Red+Red Edge+NIR region, Çeşit-1252 variety in Green+Red region, Eminbey and Mirzabey 2000 varieties in Green+Red+Red Edge were effective in band ranges in the region and showed an increase (+) in disease severity reactions.

Keywords: Wheat, Yellow rust (*Puccinia striiformis* f. sp. *tritici*), Hyperspectral data, Spectral indices, Phenological stage

Özet

Sarı pas (Etmek: *Puccinia striiformis* f. sp. *tritici*) hastalığı, buğday da üretim ve kaliteyi olumsuz yönde etkileyen önemli fungal bir hastalıktır. Bu araştırmanın amacı; test materyallerine farklı dozlarda (%0, %25, %50, %100) uygulanan sarı pas hastalığına karşı bitkinin gösterdiği reaksiyonların spektral özellikler yardımıyla belirlenmesi ve hastalığın mevsim içindeki değişimini etkileyen spektral bant bölgelerinin ortaya çıkarılmasıdır. Çalışma kapsamında, Ekmeklik çeşitler için; Eser, Bayraktar 2000 ve Demir 2000 çeşitleri erken-orta dönemde, Kenanbey çeşidi ise orta-geç dönemde yüksek korelasyon göstermiştir. Bütün ekmeklik çeşitler için etkili bant bölgesi olan Kırmızı+Kırmızı Kenar+Yakın Kızıl Ötesi (NIR) aralığında, Kenanbey çeşidi ise NIR aralığında hastalık şiddeti değerlerinde artış (+) göstermiştir. Makarnalık çeşitler için; Eminbey ve Çeşit-1252 çeşitleri erken dönemde, Mirzabey 2000 çeşidi erken-orta dönemde, Kızıltan 91 çeşidi ise orta-geç dönemde yüksek korelasyon göstermiştir. Kızıltan 91 çeşidi ise Kırmızı+Kırmızı Kenar+NIR bölgede, Çeşit-1252 çeşidi Yeşil+Kırmızı bölgede, Eminbey ve Mirzabey 2000 çeşidi Yeşil+Kırmızı+Kırmızı Kenar bölgedeki, bant aralıklarında etkili olmuş ve hastalık şiddeti reaksiyonlarında artış (+) göstermiştir.

Anahtar kelimeler: Buğday, Sarı pas (*Puccinia striiformis* f. sp. *tritici*), Çok bantlı veri, Spektral indeks, Fenolojik dönem

1. Introduction

Wheat is produced worldwide for 8000 years, is the one of basic human nutrients (carbohydrates, proteins, vitamins, minerals, fiber sources). In particular, four agricultural crops were described as accounting for half of global primary crop production in 2020: sugar cane, maize, rice and wheat (FAO, 2020). Wheat cultivated in an area of 215.9 million hectares worldwide in 2019 being Number One in the world's grain production (FAO, 2020). Plant diseases that cause unfavorable effects on crop yield and quality result economic losses in crop production. Therefore, monitoring and detection of plant diseases is critical to the sustainability of agricultural production (Strange and Scott, 2005). Rust caused by *Puccinia* sp. is an important fungal disease that causes significant yield and quality losses in wheat growing ecosystems around the world (Samborski, 1985; Roelfs, 1978). The optimum temperature for the development of yellow (stripe) caused by the *Puccinia striiformis* f. sp. *tritici* factor is 12-20°C, which is effective in the highlands of spring and early autumn, late autumn and early summer.

Many yellow rust epidemics reduced wheat yield and quality in Türkiye, especially in the rainy and cold years following spring (Dusunçeli et al. 1996). Yellow rust adversely affects early development of crops, a percentage of which can result in an economic loss of up to 70%. It is known that the yield decreases especially in susceptible varieties and lowers the quality by reducing the original size of grain (Chen, 2005). Rust is seen on leaves and spikes of wheat, even though it appears as intensive on leaves. On the upper surface of the leaf when conditions are suitable for disease development, yellow color pustules seem the form of similar to a machine sewing mark, thus it can be called "yellow or stripe rust". According to reports on the 2010 yellow rust epidemic, the disease was observed in half of the wheat growing area in Türkiye, causing a loss of 1.52 million tonnes (50-60%) in the Southeast Anatolia region (Aktaş et al. 2012). However, the extent of the rust depends on the resistance or tolerance of the wheat, the time of the first appearance of rust, the rate of disease development and the duration of the disease on the wheat. Currently, observations are taken using traditional methods (visual, tissue analysis, deep and structural methods) in yellow rust reaction evaluations. In the evaluations made, mistakes can be made at varying levels and the evaluation may take a long time. For this reason, it is imperative to develop evaluation methods whose results are trusted and completed in a short time. By using remote sensing techniques, it is possible to obtain fast and accurate information about some plant diseases and different morphological features of plant vegetation with the spectral reflection values obtained from different parts of plants (leaves, branches, seeds, soil, etc.) (Zhang et al. 2011). Advances in optical sensors and Remote Sensing technology provide the opportunity to continuously record the parameters that reveal precise and accurate results by eliminating the error arising from bias, the relationship between vegetation development in large areas and the index of biotic stress. Using a variety of simple but effective optical tools, it can detect objects or structures in a much broader spectral range than that of human observation (Hatfield and Pinter, 1993; Nicolas, 2004; Moshou et al. 2005; Qin and Zhang, 2005).

Among the various types of remote sensing techniques, hyperspectral remote sensing is the most effective method for detecting weak signals in the spectrum due to its high resolution characteristics (Goetz et al. 1985). Hyperspectral analysis can be widely used to monitor plant vitality and stress factors (Leaf Area Index-LAI, pigment coverage, plant diseases and pests, etc.) (Haboudane et al. 2004; Moshou et al. 2004; Oppelt and Mauser, 2004; Duveiller et al. 2011; Zhang et al. 2012a). For this reason, the diverse vegetation files (VI) are created to decide these with the investigations within the final period. The in situ determination of disease infections is based on the principle that different reflectance values of different morphological anomalies observed in plants on the electromagnetic spectrum can be followed with different spectral indices. Different research was performed in canopy and leaf layers to identify rust under field conditions.

These indices are broadly utilized to decide rust (*Puccinia* spp.) and *Septoria tritici* Blotch (*Zymoseptoria tritici*) at the canopy level (Zhang et al. 2012a; Liu et al. 2020; Yu et al. 2018). Sensor technology and related remote sensing techniques are based on the spectral reflectance characteristics of the plant canopy. These characteristics depend on the health of the plant during the vegetative period, the pigment and photochemical content of the leaves and their relationship to light (Merzlyak and Chivkunova, 2001). Disease or reaction can be determined by interpreting different indicators obtained as a result of evaluations made on healthy and diseased plants by using different sensors.

Wideband vegetation indices and band regions developed based on plant stress factors are commonly used to distinguish healthy plants from diseased plants to determine plant disease and reactions (Delwiche and Kim, 2000). Moshou et al. (2004) determined that the wavebands centered at 680 nm, 725 nm, and 750 nm were the most sensitive bands for yellow rust detection. The researchers reported classification accuracy of over 95% by using the Normalized Differential Vegetation Index (NDVI). Zhang et al. (2012b) reported that there was a correlation between spectral shape and spectral characteristics in certain spectral regions of yellow rust infection. Naidu et al. (2009) used the leaf reflectance values in the diagnosis of plants infected by virus. The detection of infected and uninfected leaves can be determined with an accuracy of 70% by using vegetation indices. Devadas et al. (2009) used ten vegetation indices (VIs) in their study to distinguish three different rust types. They observed that the anthocyanin reflectance index (ARI), and the Transformed Chlorophyll Absorption Reflectance Index (TCARI) have effective results in the differentiation of plant diseases.

The aim of this study was to determine yellow rust and reaction in some bread and durum wheat at different growth stages. The specific objectives of this study were to (1) Demonstrate the reflectance characteristics of infected wheat plants under artificial yellow rust epidemic conditions at different growth stages over the spectral range of 331-1141 nm; (2) to investigate the sensitivity of spectral indices to discriminate the reactions of wheat affected by yellow rust at different growth stages; (3) to develop the optimal tri-band spectral indices for discriminating yellow rust reactions in wheat at different growth stages; (4) to evaluate the performance of the newly defined indices.

As a result of this study, the effective control practices against the yellow rust in wheat can be developed by monitoring the wheat plants in effective manner with suitable tools to save wheat yield.

2. Material and Methods

2.1. Climatic and Soil Characteristics of the Field

The study was conducted in the the Field Crops Central Research Institute (TARM) during the 2018-2019 growing season in Yenimahalle/Ankara/Türkiye (Figure 1). The climate data for the period in which the study was conducted are given in Table 1. The monthly total precipitation was 33.2 mm and the monthly average temperature was 12.08 °C. The soil texture was found to be clayey-loamy.

Figure 1. The research area (TARM) in Yenimahalle / Ankara



Table 1. The monthly climate data of Yenimahalle (Ankara) location in 2018-2019 growing season

Climatic Data	Months (2018 Year)					Months (2019 Year)							Mean
	XIII	IX	X	XI	XII	I	II	III	IV	V	VI	VII	
Average Temperature (°C)	25.0	20.0	14.94	9.0	3.3	2.0	4.8	7.2	10.8	18.2	22.4	23.1	12.08
Highest Temperature, (°C)	32.0	33.2	21.65	23.5	12.6	10.8	15.8	20.4	25.5	34.2	33.4	34.9	24.43
Lowest Temperature, (°C)	18.0	8.1	9.43	-2.3	-10.2	-10.4	-2.4	-3.3	-0.9	6.1	11.7	10.7	0.71
Precipitation, (mm)	10.0	7.4	1.57	24.9	60.4	40.6	33.2	38.0	28.9	30.8	37.4	30.4	33.2
Relative humidity, %	37.0	46	69.83	65	81	79	70.2	55.4	42.5	47.2	52.1	42.0	58.04
Windy Speed, m/s ⁻¹ (2 m)	2.0	2.1	2.2	1.6	1.5	1.7	2.0	2.1	1.3	1.3	1.6	1.8	1.7

2.2 Plant Material

Four bread and four durum wheat varieties were used in this study. The varieties were registered by Central Research Institute of Field Crops (TARM), the years of registration and their reactions to yellow rust reactions are summarized in Table 2. Little Club was used as a susceptible control genotype. The Little Club was planted both among the materials and around the research area. By using this method, it was possible to simultaneously collect spectral data on susceptible and resistant cultivars to yellow rust and to form reaction groups and to compare within and between groups.

Table 2. Varieties used in the study, year of registration and disease reaction

Bread Group			Durum Group		
Variety	Registration Year	Disease Reaction	Variety	Registration Year	Disease Reaction
Bayraktar 2000	04.28.2000	Moderate Susceptible	Çeřit-1252	04.26.2000	Moderate Susceptible
Demir 2000	04.28.2000	Susceptible	Eminbey	04.06.2009	Resistant
Eser	05.02.2003	Resistant	Kızıltan 91	04.26.1991	Moderate Susceptible
Kenanbey	04.06.2009	Susceptible	Mirzabey	04.28.2000	Moderate Susceptible

2.3 Experiment Design and Sampling

All test material seeds were sown on October 15, 2018. All plant materials were inoculated with yellow rust urediospores 0%, 25%, 50%, and 100% doses on 15 April 2019 by using urediospores to induce different indices of yellow rust (Table 3). The experimental design was planted according to the four-factor urediospores application doses for bread and durum varieties randomized trial design. The trial consisted of 8 blocks in total, including 2 blocks that were not inoculated with urediospores and six blocks with disease inoculation at 25%, 50%, and 100% spore. Each block consisted of 3 replications and 1 m and 3 rows of each variety were planted. Yellow rust symptoms can be seen in early grain filling and milk production periods. For this reason, a period after the middle of May (25 May 2019), which is the milk-filling period, was chosen depending on the location's feature to take spectral measurements.

Table 3. Experimental design for yellow rust (YR) urediospores application dose

Replication 1	YR (Dose 0%)		YR (Dose 25%)		YR (Dose 50%)		YR (Dose 100%)	
	Bread	Durum	Bread	Durum	Bread	Durum	Bread	Durum
Replication 2	YR (Dose 0%)		YR (Dose 25%)		YR (Dose 50%)		YR (Dose 100%)	
	Bread	Durum	Bread	Durum	Bread	Durum	Bread	Durum
Replication 3	YR (Dose 0%)		YR (Dose 25%)		YR (Dose 50%)		YR (Dose 100%)	
	Bread	Durum	Bread	Durum	Bread	Durum	Bread	Durum

2.4. Methodology

2.4.1 Inoculation and Disease Reaction Determination

It is possible to reveal the vegetation indices (VI) that best correlate the disease index (DI) of diseased and non-infected plants and the band ranges to be used in their differentiation. Spore inoculation was homogenized in mineral oil (Soltrol 170®) at different application doses of yellow rust and 0% (negative control group), 25%, 50%, and 100% doses (3, 6, 12 mg/200 mL spore solution) were applied on the test materials ULV. The first inoculation was applied on May 06, 2019 (Feekes 6) which can be considered as the plant's rooting period (Large, 1954). The second inoculation of yellow rust was applied 3 pre-flowering period seven days after the first inoculation (Feekes 10), on May 13, 2019.

2.4.2 Evaluation of Disease Reactions

Evaluation of disease reactions and leaf samples were collected from the plots that were not inoculated with the disease and were inoculated for the disease, once every 7 days (on May 25, 2019, June 06, 2019, June 15, 2019) 19 days after the spore's inoculation (on May 06, 2019) (Table 4). Disease reaction evaluations were made according to different phenological periods (Feekes, Zadoks) (Large, 1954; Zadoks et al. 1974).

Table 4. Date of leaf samples and physiological period

Development Period	Sampling Dates	Physiological Period	Feekes	Zadoks Scale
Early	On May 25, 2019	Flowering Beginning (Early Period)	10.5.1	60
	On June 06, 2019	Grain Binding (Early-Middle Period)	10.5.3	69
Late	On June 15, 2019	Milk Settlement Period (Middle-Late Period)	10.5.4	71
	On June 23, 2019	Yellowing Period (Late Period)	11.1	75

Calculation of yellow rust index at leaf scale and canopy level in wheat were made by applying the multi-correlation technique and utilizing the difference in spectral reflectance values determined according to different color changes (lesions) specific to yellow rust. The current Vegetation Indexes (VI) developed by using different band combinations in this experiment design was aimed to determine the period in which the disease index was most intense.

Disease reaction evaluations on leaves were made for each variety by using a tripod at the canopy level, with the help of a spectroradiometer, and 3 spectral reaction evaluations (spectral reflection measurement). After taking the average of the values, the disease severity (%DI) value was determined with an average spectral reflectance value for each variety. The index of yellow rust (Peterson et al. 1948) and the reaction types of plants to yellow rust (Roelfs et al. 1992) were, also, recorded by using the Modified Cobb scale on the collected samples. In the susceptible control Litte Club genotype, the disease reaction was evaluated as 100S. As a result of this evaluation of susceptible control genotype, the results of the reaction tests were reliable and all the materials were evaluated.

Infection Coefficients (CI) were used to calculate the index of yellow rust (%DI) in the evaluations. The scale values of rust disease indices (%DI) on the leaf surface were used to calculate CI. The area covered by the disease on the leaf (Spectral Mixture Analysis-Image Classification-unsupervised Classification (0-100) was determined to evaluate reactions. Coefficients of Infection (CI) were classified into 5 groups according to their reactions (Immune(I): 0, Resistant(R): 0.1-5.0, Moderate resistant (MR): 5.0-20.0, Moderately susceptible (MS): 20.1-40.0, Susceptible (S): 41.0-100) (Akan, 2019). In the determination of reactions.

It is critical to determine the severity of the disease in a short period time in the automatic system to give more accurate results. This process is the first step in determining of the diseased leaf image. They were obtained (acquiring) as RGB (Red, Green, Blue) with any digital or thermal camera to accurately determine the severity of disease (% DI). As a second step, in the pre-processing of the image, Spectral evaluation of disease was randomly selected from 5 leaf samples of each variety, and, then, their pictures were taken with a digital and thermal camera.

Statistical classification methods are commonly used to classify remotely sensed images. These methods assume that similar cover types have similar spectral properties, so that they can be distinguished from each other using some estimated statistical measures (Kavzoglu and Reis, 2008). Recently, vector supported machine learning techniques have been used to increase the accuracy of land use classes by using high resolution satellite images such as RapidEye in digital applications in image processing, non-parametric statistical learning methods (Ustuner et al. 2015).

In this study, high-resolution satellite images were not used to determine the diseased areas. Diseased areas were determined on the leaf through the pictures taken with digital and thermal cameras. Classification was based on a digital image to increase verification. In the disease evaluations, the disease score reading (%) was made as a visual estimation in the first stage in the calculation of disease severity for different phenological periods. In practice, true diseased areas were determined by verifying with unsupervised classification over digital leaf images including diseased areas.

Firstly, the disease-free green areas were masked on the leaf images obtained as tri-band (Red, Green, Blue) in ".tif" format by the thermal camera, and first of all, diseased areas were identified. For this, sampling areas were determined on the diseased leaf sample, and 8 different colors were classified according to the severity of the disease by using the unsupervised classification in the "Image Classification" extension in ArcGIS 10.5 (Abburu and Golla, 2015). Areas with the same disease severity were given the same number, and as a result, areas with different colors (disease rate) were determined by spreading over the entire leaf surface. The disease severity values in each different color group were expressed as a percentage (%) by adding the pixel numbers and converting to the area, and the total % Disease Score value was obtained for the calculation of disease severity (%DI). In the calculation of the disease score (%) over the total leaf area, the blue areas (pixel number) in which the pustule formation were observed on the diseased leaf image taken with a digital camera or thermal camera were considered. The disease score (%) was determined by calculating the total number of pixels in which these areas were seen and proportioning them to the total leaf area (total number of pixels). The ratio of the total number of diseased pustules to the total leaf area was determined on the digital image using the unsupervised classification technique by using the "Image Classification module" in ArcGIS (Figure 2).

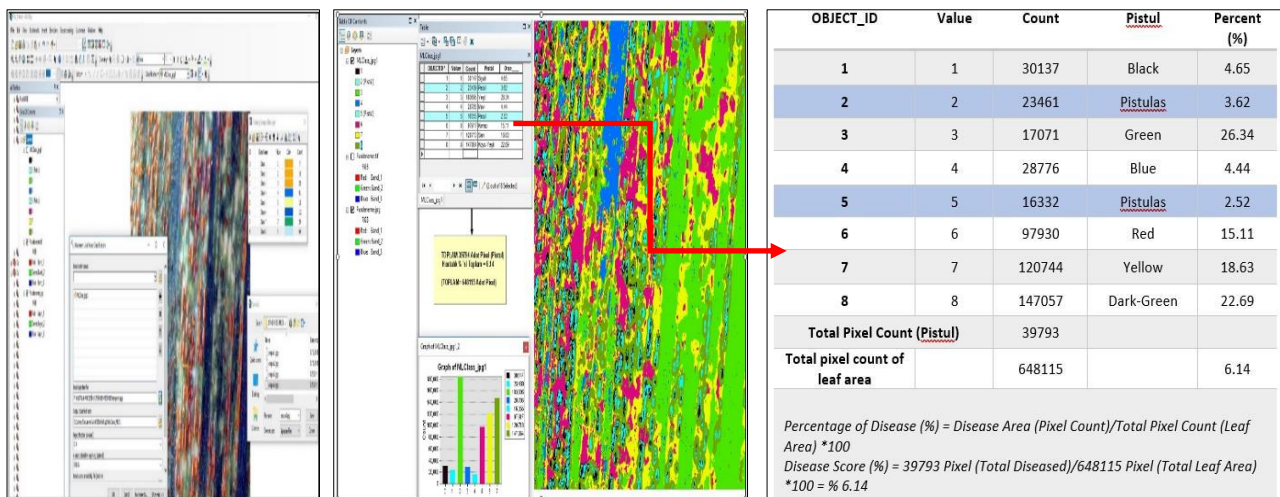


Figure 2. Revealing diseased areas with the "unsupervised classification technique" in ArcGIS

2.4.3 Generating Spectral Reflection Curves of Plants for Different Phenological Periods

Using hyperspectral remote sensing data to diagnose plant diseases and determine disease index, revealing the spectral reflection properties of wheat is important for determining index of yellow rust and its management of the disease in a timely and economical manner. The spectral reflectance of the canopy was collected with an ASD FieldSpec spectrometer (Analytical Spectral Devices, Boulder, CO, USA). All test material's canopy spectral measurements were taken at a height of 1.3 m below the soil level. A 30 cm x 30 cm Ba₂SO₄ calibration plate was used to correct the reflectance.

Healthy green plants were shown to have high absorption (low reflectance) in the visible region, as expected for the green band, and low absorption and high reflectance in the Near Infrared Region (NIR) (Nilsson, 1995). Spectroradiometric canopy reflectance measurements were taken between 11:00 and 15:00 (Istanbul local time) when the under cloudless conditions were perpendicular to the earth, by using a portable handheld Spectroradiometer device. With the help of a spectral sensor, spectral reflectance measurements were taken at 3 nm intervals with a bandwidth of 330-1150 nm at different time intervals (once a week) according to different development periods of wheat (between fraternity and milk production). Measurements were taken at a 25° angle to the soil surface and at a 25 cm height from the plant canopy surface. Measurements done by using the spectral sensor were transferred to computer environment simultaneously with cable connection. The spectroradiometer (Figure 3) used in the measurements has a single channel and includes UV/VIS/NIR band channels, and a total of 256 observations (readings) were taken, each channel being taken every 3 nm in the range of 331-1141 nm.



Figure 3. Handheld spectroradiometer used for taking canopy level spectral reflection measurements

3. Results

3.1 Determination of Sensitive Spectral Band Regions Used in Differentiating Yellow Rust in Different Phenological Development Periods

"Multi Correlation" was applied to distinguish plant samples having disease symptoms and to reveal the effective band regions in the range of 331-1141 nm in different phenological periods. It was determined that the prominent band gaps determined by using the correlation values depending on the spectral reading values on the bread and durum varieties were statistically significant (p<0.001).

Since yellow rust symptoms did not fully develop between disease index (DI) and spectral indices in the early-mid development period (beginning of flowering-Feeks 10.5.1), the correlation values were concentrated in the Green, Red, and Red Edge within the visible region, and in the middle-late (grain setting-10.5.3) and late period (milk setting period-10.5.4). Near Infrared bands were used to differentiate diseases effectively. Multi-correlation values obtained between the spectral reflectance values determined for different phenological development periods and the disease index were used for the selection of sensitive bands to be used to diagnose disease symptoms. In the early stages of phenological development, from tillering to the end of the steaming period, the difference between the spectral reflection values between the plants with and without disease symptoms is not clear. This change can be observed in the late stages of development. In the late stages of development, this separation on plants infected with yellow rust could be observed, especially on May 25, 2019, June 06, 2019 (grain filling), and June 15, 2019 (milk setting), which is the beginning of flowering.

3.2 Determination of Sensitive Spectral Band Regions Used in Differentiating Yellow Rust in Bread Wheat Varieties

In Eser variety; high correlation values were determined between 535-716 nm in the visible region and 730-1041 nm in the NIR region (Figure 4). In the early period, a high correlation was determined between the bands of 526-695 nm ($R^2=0.146$) in the Green+Red region, which is one of the visible band bands, and a high correlation in the band range of 672-796 nm in the Red Edge + NIR region in the early-mid period ($R^2=0.566$). In the mid-late period, a high correlation was found in the 726-1076 nm band in the Red Boundary+Near Infrared region ($R^2=$ When all periods were evaluated together, it was determined that the 540-716 nm band gap in the Green+Red+ RedEdge region was the most effective region in the diagnosis of disease ($R^2=0.128$) (Table 5 and Table 9). When disease variety is compared to the variety of absence of disease, high correlation values were observed in the Green and Red region bands in the early period, while low correlation values were observed in the same band intervals in the late period. In disease-free and all other phenological periods, increases in correlation values were observed starting from the Near Infrared Regions.

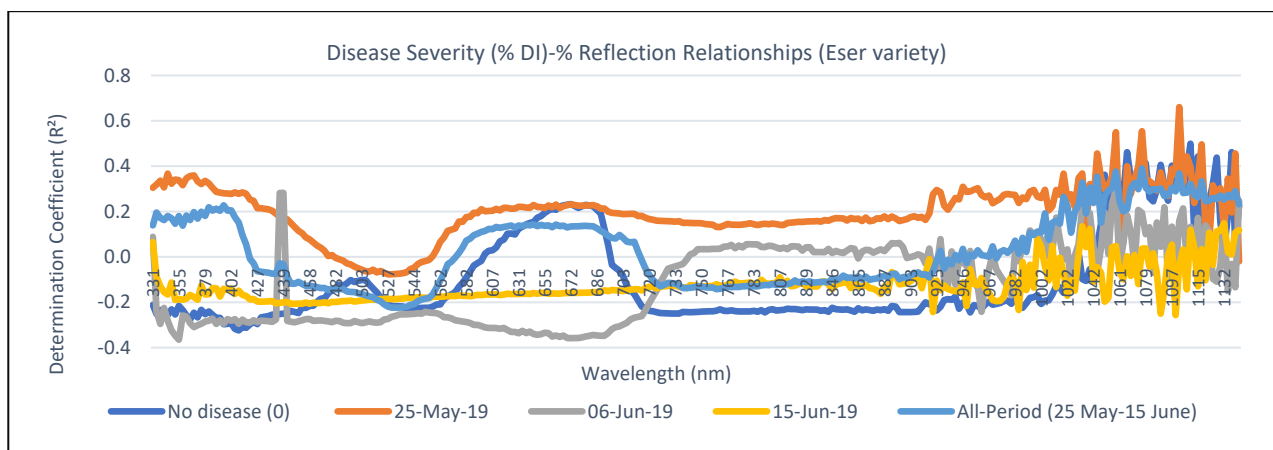


Figure 4. Disease index (%DI)-reflection (%) relationships in Eser variety

Table 5. According to phenological periods effective spectral band regions in detection of yellow rust and correlation values (determination correlation R^2) of different disease dose applications in Eser variety

Variety	Period	Application	R^2	Effective Band Range (nm)	Regression Equation	
Eser	All Period	No	0.184	535-716 730-1041	$y = 0.001x - 0.2516$	
	May 25- June 15 2019	Disease (0)				
	Early Period	May 25, 2019 (10.5.1)	25%	0.146	526-695	$y = 0.0005x + 0.118$
			50%			
			100%			
	Early-Middle Period	June 06, 2019 (10.5.3)	25%	0.566	672-796	$y = 0.0016x - 0.3479$
			50%			
			100%			
	Middle-Late Period	June 15, 2019 (10.5.4)	25%	0.409	726-1076	$y = 0.0006x - 0.2098$
			50%			
100%						
All Period	May 25-June 15, 2019 (10.5.1-10.5.4)	25%	0.128	540-716	$y = 0.0007x - 0.0692$	
		50%				
		100%				

In Kenanbey variety; it was susceptible to yellow rust in the early period, a high correlation was determined in the band range of 443-495 nm in the Blue region, 551-689 nm in the Green+Red region, and 730-1047 nm in the Red Edge +NIR region in plants without any signs of disease in the visible region (Figure 5). It was determined that the band gap of 443-537 nm ($R^2= 0.440$) was effective in the early period, and 457-695 nm of the Blue+Green+Red region bands in the Early-Middle period ($R^2=0.407$). In the mid-late period, a high correlation was found in the 915-1089 nm band gap ($R^2= 0.472$). When all the periods are evaluated together, a high correlation was found with a band gap of 544-726 nm in the Green+Red+Red Boundary region (Table 6 and Table 9). Kenanbey variety showed high correlation values in all bands of the spectroradiometer in the late period (on 15 June 2019) compared to disease-free application. It followed a stable course by showing low correlation values in the early and early-middle periods. When the whole period is evaluated together, the highest correlation values were found in the Green and Red region bands.

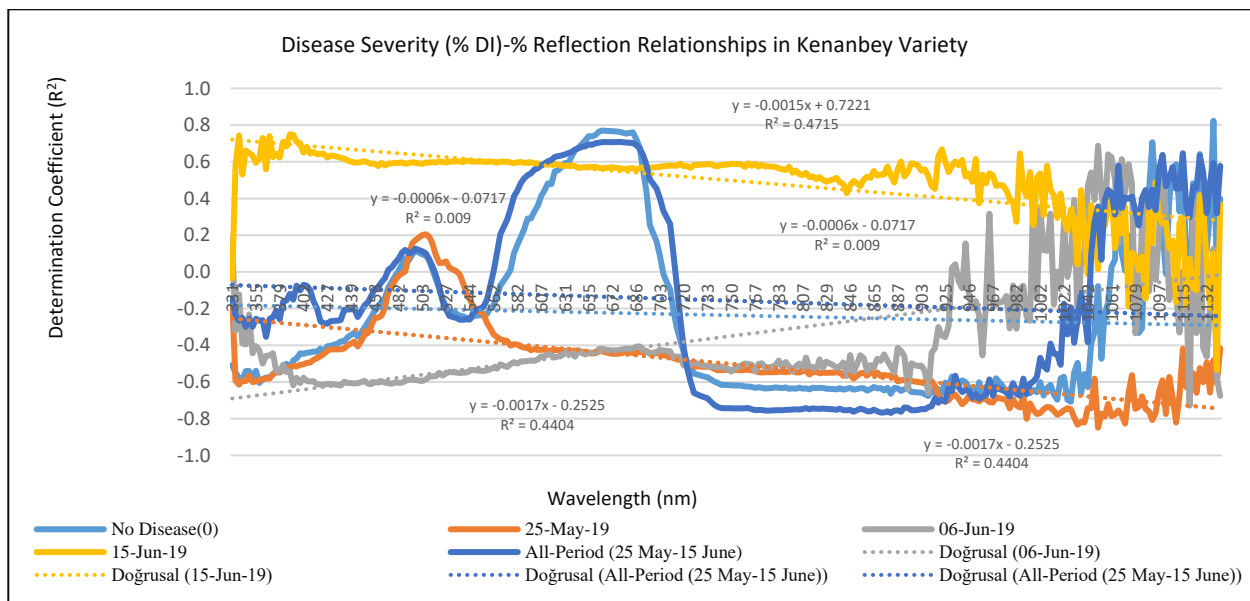


Figure 5. Disease index (%DI) - reflection (%) relations in Kenanbey variety

Table 6. Spectral band regions and correlation values effective in the detection of yellow rust in various diseases dose applications according to phenological periods in Kenanbey variety

Variety	Period	Application	R ²	Effective Band Ranges (nm)	Regression Equation
Kenanbey	All Period May 25-June 15, 2019	Not spore application (0%)	0.005	443-495 551-689 730-1047	$y = -0.0004x - 0.1804$
	Early Period May 25, 2019 10.5.1	25%	0.440	443-537	$y = -0.0017x - 0.2525$
		50%			
		100%			
	Early-Middle Period June 06, 2019 10.5.3	25%	0.407	457-695	$y = 0.0023x - 0.6925$
		50%			
		100%			
	Middle-Late Period June 15, 2019 10.5.4	25%	0.472	915-1089	$y = -0.0015x + 0.7221$
		50%			
		100%			
All Period May 25- June 15, 2019 10.5.1-10.5.4	25%	0.009	371-405 440-500 544-726	$y = -0.0006x - 0.0717$	
	50%				
	100%				

In Bayraktar 2000 variety, considering the phenological development period, it was observed that the bands of 405-500 nm in the Blue region, 558-661 nm in the Green+Red region, and 736-1038 nm in the Near Infrared Region were found to be effective in the visible region for plants without disease symptoms (Figure 6). It was observed that the band gap of 409-570 nm in the Blue+Green region in the visible region was effective for the determination of disease indices in the early development period ($R^2= 0.094$). In the early-middle period (on June 06, 2019), the band gap of 670-775 nm, which includes the Red+Red Boundary+Near Infrared region, was effective ($R^2= 0.671$). It was found to be effective in the 842-1058 nm band range in the NIR region in the Mid-Late period ($R^2 = 0.519$).

When all periods are evaluated together, it was determined that the most effective region in the diagnosis of the disease was 368-409 nm in the Blue region, 415-502 nm in the Blue+Green region and the 551-716 nm band regions in the Green+Red+Red Edge region (Table 7 and Table 9). Bayraktar variety showed high correlation in all spectral band regions in the late period, followed a stable course up to the NIR region bands in the early and early-mid periods and showed an increase in correlation values again from this region.

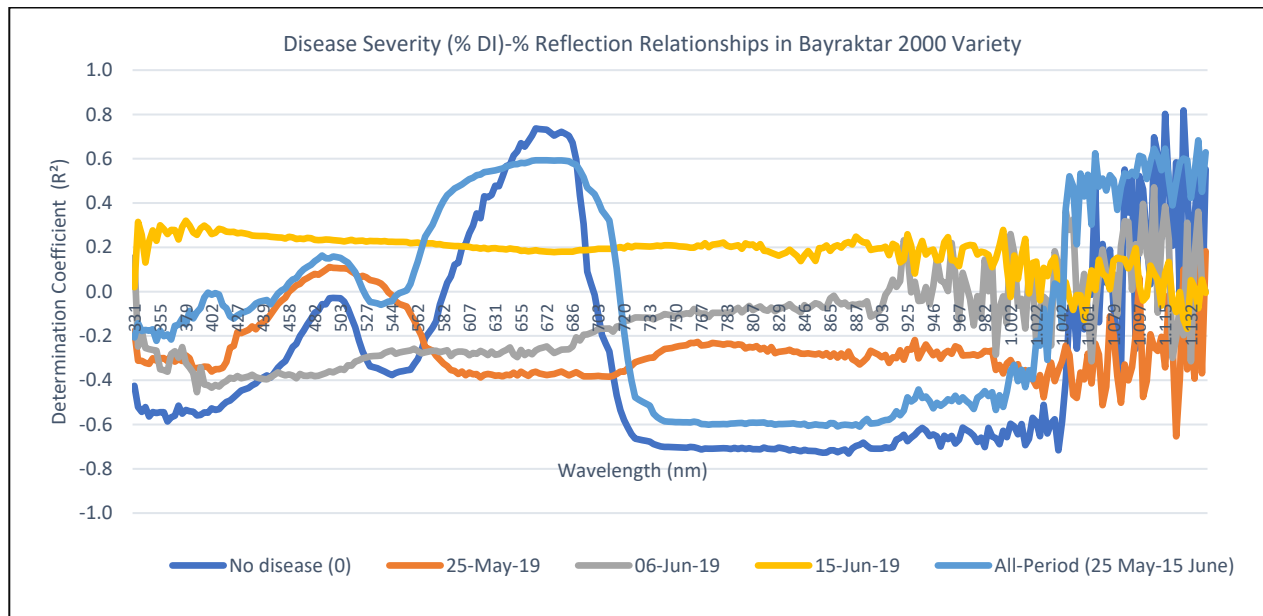


Figure 6. Disease severity (%DI)-reflection (%) relations in Bayraktar 2000 variety

Table 7. Spectral band regions and correlation values effective in the detection of yellow rust in various diseases dose applications according to phenological periods in Bayraktar 2000 variety.

Variety	Period	Application	R ²	Effective Band Ranges (nm)	Regression Equation
Bayraktar 2000	All Period 25 May-15 June 2019	Not spore application (0%)	0.005	405-500	y = -0.0005x - 0.29
				558-661	
				736-1038	
				443-537	
	Early Period May 25, 2019 10.5.1	25%	0.094	409-570	y = -0.0005x - 0.1795
		50%			
		100%			
	Early-Middle Period June 06, 2019 10.5.3	25%	0.671	670-775	y = 0.0018x - 0.4076
		50%			
100%					
Middle-Late Period June 15, 2019 10.5.4	25%	0.519	842-1058	y = -0.0007x + 0.2835	
	50%				
	100%				
All Period May 25-June 15, 2019 10.5.1-10.5.4	25%	0.0047	368-409	y = -0.0004x - 0.0058	
	50%				
	100%				

In Demir 2000 variety; considering the phenological development period, it was observed that the band gap of 405-549 nm in the Blue+Green region, 550-689 nm in the Green+Red region and 725-1044 nm in the Red Edge +NIR were effective for determination of plants without disease symptoms (Figure 7). It was determined that the Blue+Green region, located in the visible region, reached effective and high correlation values with a band gap of 402-558 nm in the determination of disease index in the early development period (R² = 0.122). High correlations were detected in the band range of 677-800 nm, which is located in the Red+Red Boundary+NIR region in the early-mid developmental period (R² = 0.464). In the mid-late period, the 796-1058 nm band gap of the NIR region was effective (R² = 0.112). When all the periods were evaluated together, the 364-405 nm and 433-485 nm bands of the Blue region and the 554-689 nm bands of the Green+Red region were effective (Table 8 and Table 9). While Demir variety showed low correlations in all spectral band regions in the late period, an increase was observed towards the NIR region starting from the Red region bands in the early-mid period.

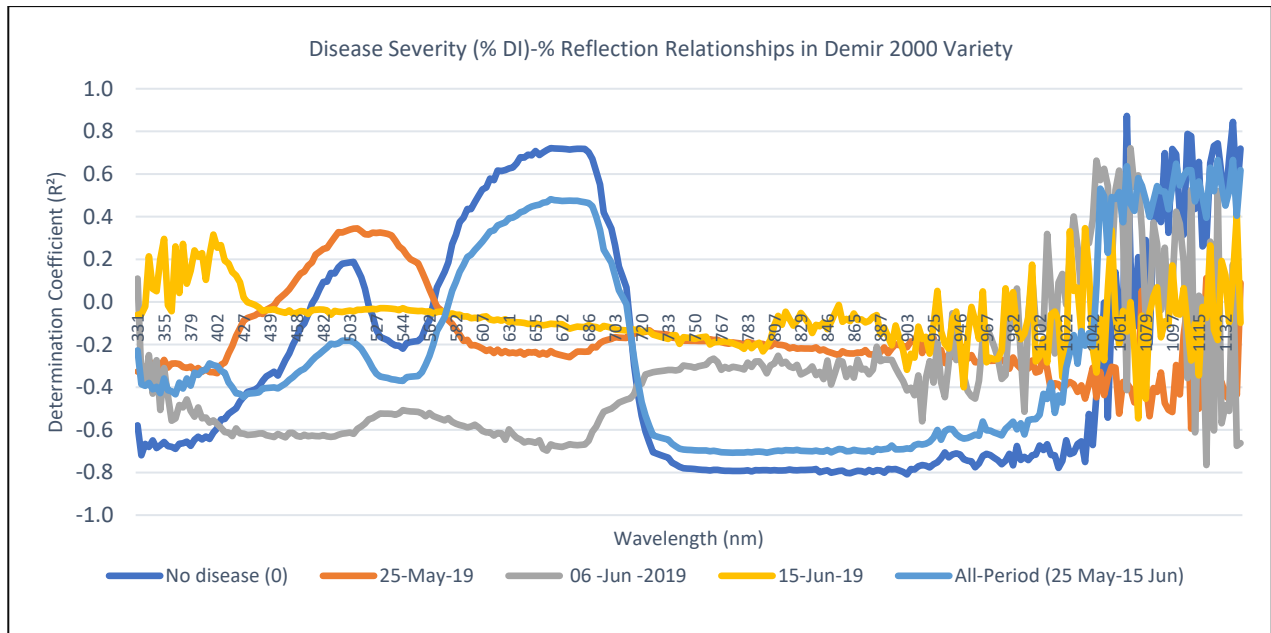


Figure 7. Disease index (%DI)-reflection relationships (%) in Demir 2000 variety

Table 8. According to phenological periods effective spectral band regions and correlation values in Yellow Rust detection of different disease dose applications in Demir 2000 variety

Variety	Period	Application	R ²	Effective Band Ranges (nm)	Regression Equation
Demir 2000	All Period May 25-June 15, 2019	Not spore application (0%)	0.001	405-549 550-689 725-1044	y = -0.0002x - 0.2237
	Early Period May 25, 2019 10.5.1	25%	0.122	402-558	y = -0.001x - 0.4295
		50%			
		100%			
	Early-Middle Period June 06, 2019 10.5.3	25%	0.464	677-800	y = 0.0025x - 0.7149
		50%			
		100%			
	Middle-Late Period June 15, 2019 10.5.4	25%	0.112	796-1058	y = -0.0005x + 0.0033
		50%			
		100%			
All Period May 25- June 15, 2019 10.5.1-10.5.4	25%	0.028	364-405 433-485 554-689	y = 0.0009x - 0.4744	
	50%				
	100%				

Table 9. Spectral band intervals (nm) used in the separation of disease index of plants with and without disease symptoms in bread wheat varieties

Bread Varieties	Visible			Near Infrared (NIR) Region		Visible+Near Infrared
	Blue 331-510 nm	Green 511-600 m	Red 601-699 nm	Red Edge 700-750 nm	Near Infrared 750-1141 nm	Blue+Green+Red+Red Edge+Near Infrared 331-1141 nm
Period	Early Period (May 25, 2019)			Late Period (June 06-15, 2019)		All Period (May 25-June 15)
Eser	526-695			672-796	726-1076	540-716 nm Green+Red+Red Edge
Kenanbey	443-537			457-695	915-1089	544-726 nm Green+Red+Red Edge
Bayraktar 2000	409-570			670-775	842-1058	551-716 nm Green+Red+Red Edge
Demir 2000	402-558			677-800	796-1058	554-689 nm Green+Red

3.3 Determination of Sensitive Spectral Band Regions Used in Differentiating Yellow Rust in Durum Wheat Varieties

In Kızıltan 91 variety, the high correlation values were found at 440-513 nm in the visible region, 561-685 nm in the Green+Red region and 987-1079 nm in the NIR region in plants without disease symptoms in the Blue+Green region (Figure 8). In the determination of disease index in the early development period, a stable course was observed in the visible region for plants with disease symptoms and the highest correlation was observed in the Blue region bands (371-415 nm) in the visible region and 675-829 nm bands in the Red+NIR region. change was determined ($R^2=0.111$). In the early-middle period, high correlation was found in the band range of 685-830 nm in the Red+Red Edge+NIR region in the visible region ($R^2=0.159$). In the mid-Late period, the disease change was highest and the highest correlation values were determined in the band range of 680-874 nm, which is located in the Red+Red Edge+NIR region ($R^2=0.181$). When all periods are evaluated together, the highest correlation change was detected in the Green+Red region in the visible region, in the band range of 533-637 nm (Table 10 and Table 14). Kızıltan 91 showed the highest correlation was seen in the Red region bands in the mid-late period. No significant change was observed in the correlation in the early and late periods.

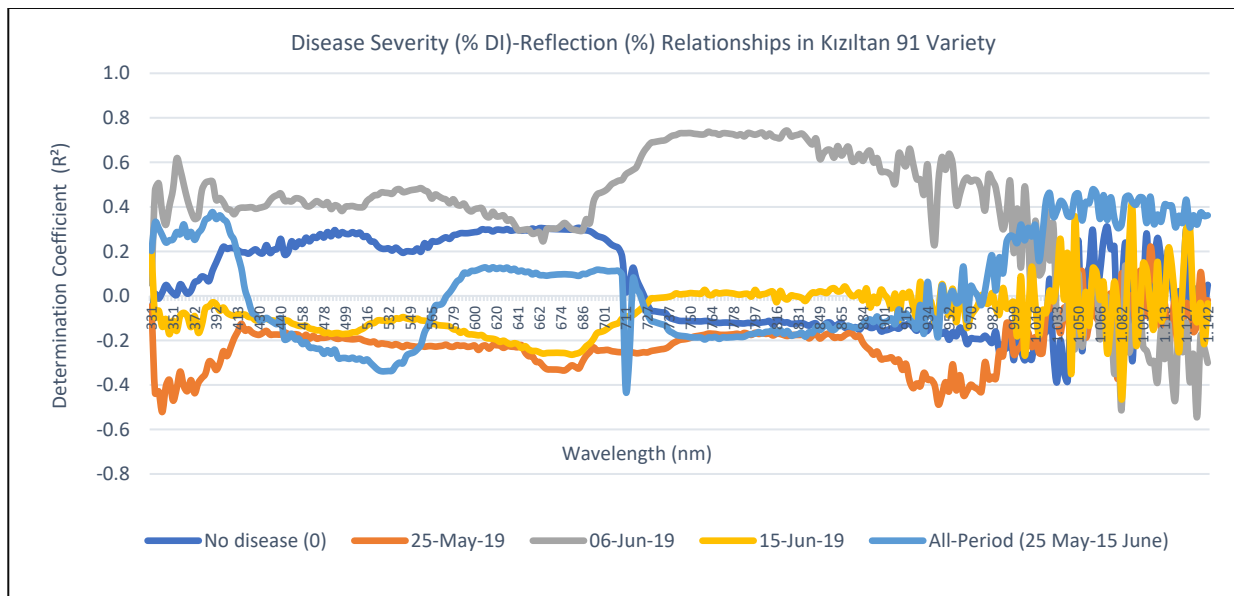


Figure 8. Disease index (%DI)-reflection relations (%) in Kızıltan 91 variety

Table 10. According to phenological periods effective spectral band regions and correlation values in the detection of yellow rust of different disease dose applications in Kızıltan 91 variety

Variety	Period	Application	R ²	Effective Band Ranges (nm)	Regression Equation
Kızıltan 91	All Period May 25-June 15 2019	Not spore application (0%)	0.324	561-685	$y = -0.0013x + 0.2434$
	Early Period May 25, 2019 10.5.1	25%	0.111	371-415	$y = 0.0004x - 0.2814$
		50%		675-829	
		100%			
	Early-Middle Period June 06, 2019 10.5.3	25%	0.159	685-830	$y = -0.0013x + 0.5903$
		50%			
		100%			
	Middle-Late Period June 15, 2019 10.5.4	25%	0.181	680-874	$y = 0.0006x - 0.1554$
		50%			
		100%			
All Period May 25- June 15, 2019 10.5.1-10.5.4	25%	0.132	533-637	$y = 0.001x - 0.1126$	
	50%				
	100%				

In Çeşit-1252 variety; low correlation at 433-516 nm, 550-640 nm in the Green+Red region, 533-725 nm in the Green+Red+NIR region and 990-1139 nm in the Near Infrared region in plants without disease symptoms observed in early visible Blue+Green region values were found (Figure 9). In determining the disease index in the early stages' development period, a stable course was observed in the visible region for plants with disease symptoms, and a high correlation was observed in the Green+Red 540-654 nm band range in the visible region ($R^2=0.371$). In the early-middle period, a low correlation in the 733-813 nm band in the Red Boundary+Near Infrared region ($R^2=0.087$) was calculated.

In the Middle-Late period, a high correlation in the Red+Red Boundary region in the 641-702 nm band range ($R^2= 0.307$) was calculated. **When all periods are evaluated together**, the highest correlation change was observed in the 865-1033 nm band within the NIR region ($R^2= 0.198$) (Table 11 and Table 14). eřit-1252 followed a stable course in all phenological periods and showed a slight increase in Green and Red region bands.

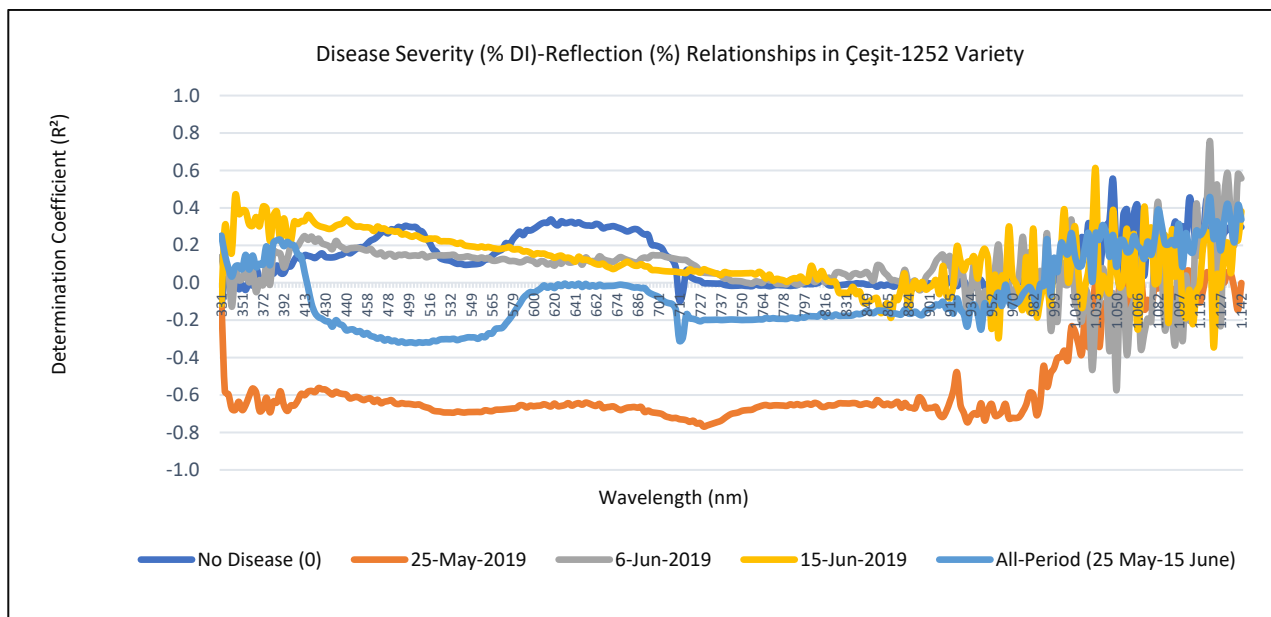


Figure 9. Disease index - % reflection relationships in the eřit-1252 Variety

Table 11. According to phenological periods effective spectral band regions and correlation values in detection of yellow rust of different disease doses in the eřit-1252 variety

Variety	Period	Application	R ²	Effective Band Ranges (nm)	Regression Equation
eřit-1252	All Period May 25- June 15, 2019	Not spore application (0%)	0.002	550-640	$y = -0.00005x + 0.13$
	Early Period May 25, 2019 10.5.1	25%	0.371	540-654	$y = 0.0016x - 0.7982$
		50%			
		100%			
	Early-Middle Period June 06, 2019 10.5.3	25%	0.087	733-813	$y = -0.0005x + 0.1478$
		50%			
		100%			
	Middle-Late Period June 15, 2019 10.5.4	25%	0.307	641-702	$y = -0.001x + 0.2605$
		50%			
		100%			
All Period May 25- June 15, 2019 10.5.1-10.5.4	25%	0.198	865-1033	$y = 0.001x - 0.2086$	
50%					
100%					

In Eminbey variety; low correlation values were determined at 549-682 nm in the Green+Red region and at 1016-1115 nm in the Near Infrared Region in plants without any signs of disease in the early period (Figure 10). **In the early period**, the highest correlation values were determined in the visible region, in the Green+Red+Red Boundary region, in the band range of 575-736 nm ($R^2= 0.523$). Increases in disease index occurred at all disease administration doses (25%, 50%, 100%). The highest increase in disease index was determined at the 100% application dose (+335.52%), followed by 50% (+287.13%) and 25% (+141.95%) dose applications, respectively. **In the determination of disease index in the early-mid development period**, a stable change was observed within the visible region for diseased plants, and a high correlation variation was detected in the Blue region bands (673-803 nm) in the visible region ($R^2= 0.132$). In this period, the increase in disease index in all disease application doses was +58.83% compared to plants without disease symptoms in disease index values. **In the Mid-Late period**, a high correlation in the 829-1004 nm band in the Near Infrared region ($R^2= 0.214$) was found. In this period, the increase in disease index was seen as +25.0% at 50% and 100% disease administration doses. **When all periods are evaluated together**, the highest correlation change was found in the visible region, in the Green+Red+ Red Edge region, within the band gap of 526-712 nm ($R^2= 0.040$).

The maximum change in disease index was observed at 100% disease dose (+17.56%), 50% disease dose (+16.89%) and 25% disease dose (+13.78%) (Table 12 and Table 14). Eminbey variety followed a stable course in all regional bands and showed a slight increase from the Red region bands in the early-mid period.

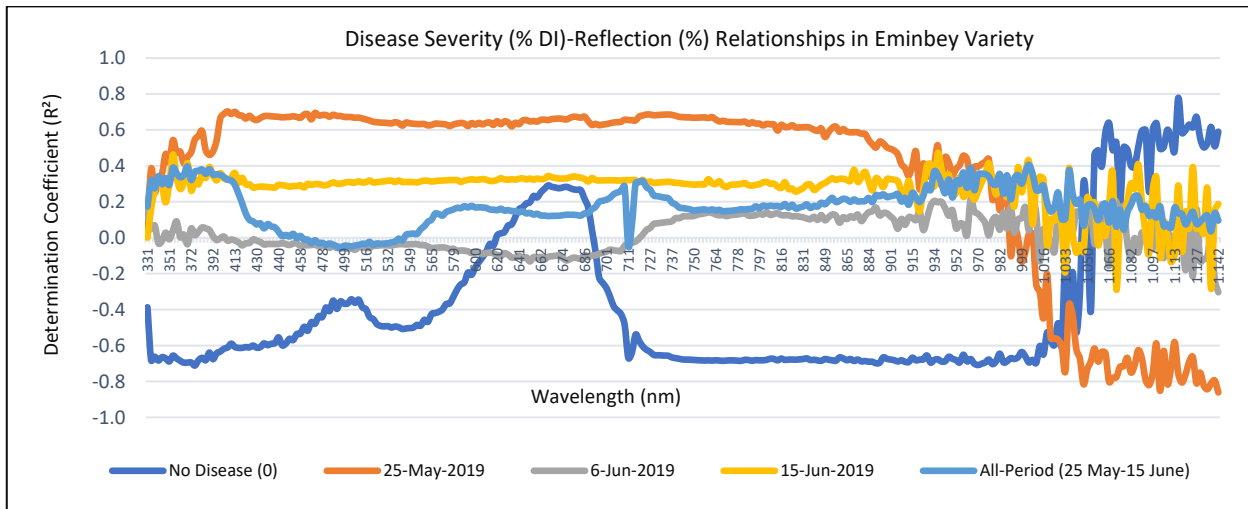


Figure 10. Disease index- reflection (%) relations in Eminbey variety

Table 12. According to phenological periods spectral effective band regions and correlation values in the detection of yellow rust of different disease dose applications in Eminbey variety

Variety	Period	Application	R ²	Effective Band Ranges (nm)	Regression Equation
Eminbey	All Period May 25- June 15, 2019	Not spore application (0%)	0.113	419-506 549-682 1016-1115	y = 0.0017x - 0.6142
	Early Period May 25, 2019 10.5.1	25%	0.523	575-712	y = -0.0042x + 0.9792
		50%			
		100%			
	Early-Middle Period June 06, 2019 10.5.3	25%	0.132	673-803	y = 0.0004x - 0.0405
		50%			
		100%			
	Middle-Late Period June 15, 2019 10.5.4	25%	0.214	829-1004	y = -0.0006x + 0.3619
		50%			
		100%			
All Period May 25- June 15, 2019 10.5.1-10.5.4	25%	0.040	526-712	y = 0.0003x + 0.1329	
	50%				
	100%				

In Mirzabey 2000 variety; in the early period, a stable course was observed throughout the visible region, and disease correlation values showed a high correlation in the range of 575-680 nm in the Green+Red region bands (Figure 11). It followed a stable course again up to the 1024 nm band gap in the Near Infrared Region, and a high correlation was determined in the band gap from this point to 1084 nm ($R^2 = 0.330$). In the determination of disease index in the early period, it was determined that there was a high correlation in the 334-381 nm band range (Blue band) located in the visible region for plants with disease symptoms ($R^2 = 0.433$). During this period, the increases in disease index were detected in all disease administration doses (25%, 50%, 100%). These increases were observed at the maximum application dose of 100% (+100%), at 50% application dose (+66.67%) and 25% application dose (+33.33%), respectively. It was determined that the Green+Red+Red Boundary bands within the visible region are effective in the 544-736 nm range ($R^2 = 0.437$). In this period, the greatest increase in disease index was observed at 25% disease dose (+66.67%) compared to plants without any disease symptoms, followed by 50% disease dose (+65.0%) and 100% disease dose (+20.0%), respectively. In the Mid-Late period, the band gap of 699-893 nm, located in the Red+Red Boundary+NIR region, was determined to be effective. The highest increase in disease index was observed at 50% disease dose (+39.71%) compared to plants having no signs of disease in the mid-late period, and a decrease was determined at other application doses. When all periods are evaluated together, the band range of 760-971 nm within the NIR region showed a high correlation change ($R^2 = 0.401$) (Table 13 and Table 14). Mirzabey variety showed a slight increase in correlation values in the Red region bands in all phenological periods, and generally followed a stable course.

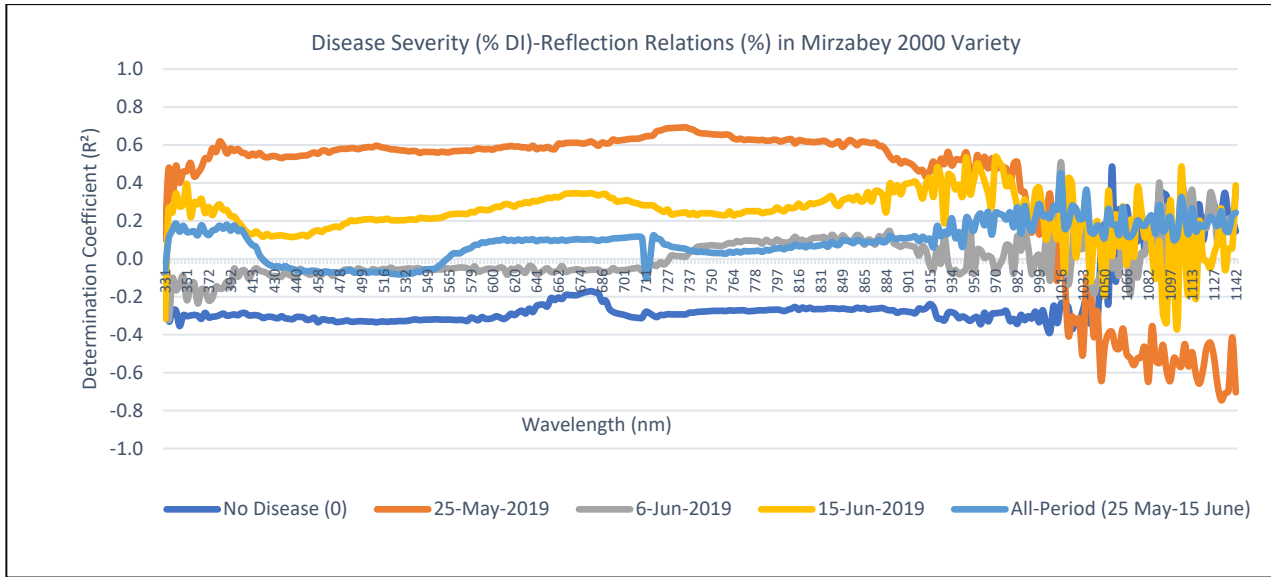


Figure 11. Disease index (DI%) - reflection (%) relationships in the Mirzabey 2000 variety

Table 13. According to phenological periods effective spectral band regions and correlation values in detection of yellow rust of different disease doses in Mirzabey 2000 variety

Variety	Period	Application	R ²	Effective Band Ranges (nm)	Regression Equation
Mirzabey 2000	All Period 25 May-15 June 2019	Not spore application (0%)	0.330	419-506 575-680 1016-1115	y = 0.0011x - 0.3946
	Early Period 25 May 2019 10.5.1	25%	0.433	334-381	y = -0.0031x + 0.8464
		50%			
		100%			
	Early-Middle Period 06 June 2019 10.5.3	25%	0.437	544-736	y = 0.0009x - 0.1269
		50%			
		100%			
	Middle-Late Period 15 June 2019 10.5.4	25%	0.0035	699-893	y = -9E-05x+0,2515
		50%			
		100%			
All Period 25 Mayıs-15 Haziran 2019 10.5.1-10.5.4	25%	0.401	760-971	y = 0.0007x + 0.0146	
	50%				
	100%				

Table 14. Spectral band Intervals (nm) used in distinction of disease index of diseased and non-disease plants in durum wheat varieties

Durum Varieties	Visible			Near Infrared (NIR) Region		Visible+Near Infrared
	Blue 331-510 nm	Green 511-600 nm	Red 601-699 nm	Red Edge 700-750 nm	Near Infrared 750-1141 nm	Blue+Green+Red+Red Edge+Near Infrared 331-1141 nm
Period	Early Period (May 25, 2019)			Late Period (June 06-15, 2019)		All Period (May 25-June 15)
Kızıltan 91	371-415		675-829	685-830	680-874	533-637 Visible Region (Green+Red)
Çeşit-1252		540-654		733-813	641-702	865-1033 Near Infrared
Eminbey		575-712		673-803	829-1004	526-712 Red+Near Infrared
Mirzabey 2000	334-381	544-736		699-893	760-971	531-719 Green+Red

Accuracy of Classification (Accuracy Assessment)

The Kappa (χ) coefficient, which summarizes the information provided by the error matrix, is used as a statistical measure that predominantly calculates the accuracy of classification. Kappa value was calculated based on disease severity (% DI) values for bread and durum varieties. In order to test the accuracy of the classified image, sample plots were selected from bread and durum wheat materials, and disease severity values (%DI) were visually read, and the obtained readings values were compared with the disease reading values obtained from the classified image. For this aim, a total of 200 sampling points were determined for bread and durum varieties. 86 readings in bread varieties and 80 readings in durum varieties matched one-to-one with the classification values. The General Accuracy Rates were 65.83% with Kappa value (X) 0.449 for bread varieties, and 61.87% with Kappa value (X) 0.423 for durum wheat varieties (Table 15). In general, Kappa grade represents 0-20% poor, 20-60% moderate, grade accuracy 60-80% good and 80-100% very good.

Table 15. Calculation of error matrix for bread and durum varieties (Accuracy Assessment) bread varieties

Bread Varieties	Observed Parcel Data (%DI) (Total)	Data from Classification (%DI) (Total)	Number of correct	Producer Accuracy (%)	User Accuracy (%)	Kappa values
Eser	24	26	19	79.17	73.08	0.460
Bayraktar 2000	31	34	26	83.87	76.47	0.482
Kenanbey	32	37	27	84.38	72.97	0.460
Demir 2000	15	23	14	93.33	60.87	0.384
Total	100	120	86	85.19	70.85	0.447
Rate of General Accuracy (RGA) = 65.83% - Average Kappa Coefficient (χ) = 0.449						

Durum Varieties	Observed Parcel Data (%DI) (Total)	Data from Classification (%DI) (Total)	Number of correct	Producer Accuracy (%)	User Accuracy (%)	Kappa values
Kızıltan 91	23	28	20	86.96	71.43	0.450
Eminbey	33	32	26	78.79	81.25	0.512
Çeşit-1252	28	35	21	75.00	60.00	0.378
Mirzabey 2000	16	25	13	81.25	52.00	0.328
Total	100	120	80	80.50	66.17	0.417
Rate of General Accuracy (RGA) = 61.87% - Average Kappa Coefficient (χ) = 0.423						

*%DI Disease Intensity

With our findings, the presence of disease, its description methods, the influenced area, effective indices and band intervals for bread varieties are summarized below;

For bread varieties; apart from Kenanbey, Eser, Bayraktar 2000, and Demir 2000 varieties showed a high correlation in the early-mid period, while the Kenanbey variety showed a high correlation in the mid-late period, the effective band area for all bread varieties was in the range of Red+Red Edge+NIR, while Kenanbey variety was Near Infrared range and an increase in disease index values (+) was observed. The list of vegetation indices used in the differentiation of disease-inoculated and disease-inoculated plants and their areas of influence are given below (Table 16).

Table 16. Vegetation indices used in the distinction of diseased and disease-free plants

Vegetation indices	Description	Formula	References	Area of Influence
NBNDVI	Narrow-Band Normalized Difference Vegetation Index	$(R_{850} - R_{680}) / (R_{850} + R_{680})$	Thenkabail et al. 2000	Following Vegetation
NRI	Nitrogen Reflectance Index	$(R_{570} - R_{670}) / (R_{570} + R_{670})$	Filella et al. 1995	Nitrogen Status
TCARI	The Transformed Chlorophyll Absorption and Reflectance Index	$3 \times [(R_{700} - R_{675}) - 0.2 \times (R_{700} - R_{550}) \times (R_{700}/R_{670})]$	Haboudane et al. 2002	Chlorophyll a + b Concentration
PhRI	Physiological Reflectance Index	$(R_{550} - R_{531}) / (R_{550} + R_{531})$	Gitelson et al. 2001	Calculating Light Usage Efficiency
NPCI	Normalized Pigment Chlorophyll Ratio Index	$(R_{680} - R_{430}) / (R_{680} + R_{430})$	Kim et al. 1994	Pigment Concentration
CARI	Chlorophyll Absorption Ratio Index	$((aR_{670} + R_{670} + b) / (a^2 + 1)^{1/2}) \times (R_{700}/R_{670})$ a = $(R_{700} - R_{550})/150$, b = $R_{550} - (a \times 550)$	Zarco-Tejada et al. 2005	Calculating Chlorophyll Absorption

Table 16. Continued

Vegetation Indices	Description	Formula	References	Area of Influence
GI	Green Index	R_{554}/R_{677}	Broge and Leblanc, 2001	Pigment Concentration
PSRI	Plant Senescence Reflectance Index	$(R_{680} - R_{500})/R_{750}$	Merzlyak et al. 1999	Pigment Coverage, Leaf Maturation and Yellowing
RVSI	Red Edge Vegetation Stress Index	$RVSI = [(R_{712} + R_{752})/2] - R_{732}$	Merton and Huntington, 1999	Internal Structure Parameters
WI	Water Index	$WI = R_{900}/R_{970}$	Peñuelas et al. 1997	Calculation of Changes in Water Amount
LCCI	Leaf and Canopy Chlorophyll Index)	$LCCI = (R_{750} - R_{705}) / (R_{750} + R_{705})$	Gitelson and Merzlyak, 1994	Calculating Chlorophyll Absorption
NVI	New Vegetation Index	$NVI = (R_{777} - R_{747}) / (R_{673})$	Gupta et al. 2001	Calculating Chlorophyll Absorption
GNDVI	Green Normalized Difference Vegetation Index	$GNDVI = (R_{750} - R_{550}) / (R_{750} + R_{550})$	Gitelson et al. 1996	Leaf Area Index, Photosynthetically Active Radiation (PAR), or Biomass (PAB)
SRPI	Simple Ratio Pigment Index	$SRPI = R_{430} / R_{680}$	Peñuelas et al. 1994	Pigment Concentration
MSR	Modified Simple Ratio Index	$MSR = (R_{800}/R_{670} - 1) / \sqrt{R_{800}/R_{670} + 1}$	Chen and Cihlar, 1996	Leaf Area Index Calculation
YRI	Yellow Rust Index	$YRI = (R_{730} - R_{419}) / (R_{730} + R_{419}) + 0.5R_{736}$	Huang et al. 2014	Wheat Disease

For durum varieties; It showed high correlation in the early period in Eminbey and eřit-1252 varieties, in the early-middle period in Mirzabey 2000 variety, and in the mid-late period in Kızıltan 91 variety. It was effective in the band gaps in the Red+Red Edge+NIR region for the Kızıltan 91 variety, the Green+Red region for the eřit-1252 variety, the Green+Red+Red Edge region for the Eminbey variety, and the Green+Red+Red Edge region for Mirzabey 2000 variety, and increased (+) disease index reactions was determined. Prominent indexes for durum varieties; SRPI, TCARI, NRI, MSR, LCCI, NPCI, NBNDVI, PSRI, PR (Table 17).

Table 17. Sensitive spectral band regions and indices effective in monitoring disease indices of different disease application doses in bread and durum wheat varieties according to phenological periods

Varieties	Spore Doses (%)	R ²	Band Ranges (nm)	Effective Band Region	Effective Period	%DI	Effective Indices	Correlation Ranges (R ²)
Eser	25%, 50%, 100%	0.566	672-796	Red+Red Edge+NIR	Early-Middle	+	NPCI, SRPI, PSRI, NRI, GI	0.256-0.212
Kenanbey	25%, 50%, 100%	0.472	915-1089	Near Infrared Region	Middle-Late	+	NRI, GI, MSR, YRI	0.521-0.380
Bayraktar 2000	25%, 50%, 100%	0.671	670-775	Red+Red Edge+NIR	Early-Middle	+	PhRI, NPCI, SRPI, GNDVI, GI	0.399-0.274
Demir 2000	25%, 50%, 100%	0.464	677-800	Red+Red Edge+NIR	Early-Middle	+	PhRI, NPCI, SRPI, RVSI, WI	0.288-0.222
Kızıltan 91	25%, 50%, 100%	0.181	680-874	Red+Red Edge+NIR	Middle-Late	+	SRPI, NPCI, PSRI, LCCI, NBNDVI	0.514-0.472
eřit-1252	25%, 50%, 100%	0.371	540-654	Green+Red	Early	+	TCARI, NBNDVI, NVI, CARI, LCCI	0.442-0.413
Eminbey	25%, 50%, 100%	0.523	575-712	Green+Red+Red Edge	Early	+	NRI, PSRI, ARI, GI, NPCI	0.607-0.402
Mirzabey 2000	25%, 50%, 100%	0.437	544-736	Green+Red+Red Edge	Early-Middle	+	WI, MSR, NDVI, NBNDVI, CARI	0.480-0.457

Within the scope of the study, sensitive band areas to be used in within the exploring of yellow rust at the end of the stem and the starting of blooming (10.5.1) are in the visible (visible) region for bread wheat varieties, (Red+Red Edge) 619-767 nm, grain filling and sensitive band areas to be used in the late period (10.5.3-10.5.4) including the milk production period, in the range of 820-1070 nm within the Near Infrared region, and in within early period (10.5.1) for durum varieties. It was determined that the band range of 586-733 nm in the Green+Red+Red Edge region, and in the late period (10.5.3-10.5.4) and 768-951 nm in the Near Infrared Region is remarkable (Table 18).

Table 18. Effective spectral band ranges (nm) determined by using reflectance values for disease detection at different yellow rust spore doses (0%, 25%, 50%, 100%) in bread and durum varieties

	Varieties	Band Intervals by Regions (nm)	
		Visible	Near Infrared (NIR)
Bread	Eser	672-796	726-1076
	Kenanbey	457-695	915-1089
	Bayraktar 2000	670-775	842-1058
	Demir 2000	677-800	796-1058
	Mean	619-767	820-1070
Durum	Kızıltan 91	685-830	680-874
	Çeşit-1252	540-654	865-1033
	Eminbey	575-712	829-1004
	Mirzabey 2000	544-736	699-893
	Mean	586-733	768-951

4. Discussion

The most obvious symptoms seen in winter wheat with yellow rust are signs within the shape of yellow machine stitches on green leaves and some parameters such as biomass, morphological and physiological parameters that cause changes in the chlorophyll and water contents. (Feng et al. 2016; Zhao et al. 2004). The basis for diagnosing plant diseases based on optical properties is based on the contrast between the spectral characteristics of healthy and infected plants. Within the scope of the study, sensitive band regions that can be used to diagnose yellow rust at distinctive development stages were determined in some bread and durum wheat varieties. Depending on the increasing amount of disease spores in the later stages of development, these spores can cause significant changes in pigment and water concentrations and canopy structure in wheat. Due to the increasing effect of the disease on the plant, a change in leaf color is observed depending on the increasing pustules and lesions (Devadas et al. 2009; Zhang et al. 2011). The sensitive wavelength changes during grain filling and milk setting are in the range of the visible and Near Infrared Regions. Within the assurance of yellow rust, deformations in the leaf structure are less in the early-mid development period when compared to the mid-late period (Devadas et al. 2009). Therefore, diseased plants in early to mid-season are less susceptible to Near Infrared region bands than mid-late plants. In some studies, on the subject, it was reported that the most effective indices used at the canopy level in detecting yellow rust by remote sensing methods were ARI (700-550 nm) and PRI (570-531nm) (Devadas et al. 2009; Huang et al. 2007).

It is known that these records have a critical part within the discovery of photosynthetic changes. The PRI indices, which employments 525 nm, 570 nm and 705 nm groups within the delicate range within the early-mid advancement period, can be used to distinguish yellow rust. The 570 nm and 525 nm bands in the Green region are related to photosynthesis in the plant, affect the chloroplasts and are remarkable in the deterioration of chloroplasts. Therefore, these region bands trigger spectral features in the plant. The 526 nm band region is the region where chlorophyll and carotenoids are strongly absorbed for photosynthetic activity in the plant. The 705 nm band, found within the Red Edge locale, is a pointer of the stress reaction made within the plant. Due to disease infection in the plant, canopy density and leaf area vary in the Near Infrared region. In this case, the Near Infrared region is a sensitive region for changes in canopy structure. Especially in the Near Infrared region, the 860 nm and 790 nm bands can be used to predict changes in canopy structure and differences in photosynthesis. The bands in the Red Edge region (700-750 nm) can be used to determine parameters such as vegetation progress, growth, moisture status, leaf area. The 750 nm band in the Red Edge region was used to distinguish diseased wheat from healthy wheat in the mid-late development period. These results are consistent with Bravo et al. (2003) in research results (750±10 nm and 861±10 nm). Similarly, Yu et al. (2018) reported that the Red Edge hyperspectral narrow bands in the Near Infrared region are effective in the differentiation (diagnosis) of diseases in vegetation. This method can be a guide for determining and controlling two- and three-band spectral indices for wheat rust monitoring in the early-mid growth stage and estimating crop losses in the mid-late period.

The present study was carried out simultaneously at the Central Research Institute of Field Crops Ankara Yenimahalle location to primarily test the reactions of some bread and durum varieties to yellow rust for different phenological periods and to determine the effects of different disease dose applications on disease development. In this study, 4 bread varieties (Eser, Bayraktar 2000, Kenanbey, Demir 2000) and 4 durum wheat varieties (Kızıltan 91, Çeşit-1252, Eminbey, Mirzabey 2000) known to have different reactions to the disease were used. Observation at different growth stages is important in monitoring plant diseases. For this reason, within the scope of the study, the development of the disease was evaluated by dividing the growth stages into four stages.

The first of these stages is the beginning of early flowering (25.05.2019, DAS-191 (Days After Sowing), the second, grain filling early-middle (06.06.2019, DAS-203) third, the period of milk formation (15.05.2019 term, DAS-212), and the late period fourth yellowing (23.06.2019, DAS-229). In order to determine the disease reactions, control (no disease application) and three different disease application (25%, 50%, 100%) doses were inoculated into the plant material. In the test material, the disease index and spectral reflectance values were evaluated simultaneously in four periods and recorded in the database. Disease reaction evaluations were made for each period within themselves by one-way ANOVA analysis of variance, and the effects of different disease dose applications on the disease reaction were evaluated at the variety level. Graphs showing the relationships between the disease index values determined depending on the different observed disease application doses and the spectral reflectance values collected simultaneously with the handheld spectroradiometer were created. In addition, multiple correlations between disease index and spectral indices were determined to determine the band gaps of the spectral regions that attract attention in disease development for different phenological periods and in which the stress relations between diseased and non-diseased plants are best expressed, and the spectral indices that correlate these band regions. Charts shows the relationships (Multiple Correlation) between Disease index (DI%) - reflection (%) for each variety. In the prediction of the disease, it was evaluated that the visible region bands in the early and early-middle (flowering onset-grain filling) development period and the Near Infrared Region in the mid-late period are more determinative in bread and durum varieties. The mid-late period (milking and yellowing) was effective in estimating crop losses. Sensitive varieties most affected by different disease dose applications; Bayraktar for bread varieties and Eminbey for durum wheat varieties. It was determined that two growth stages were effective in estimating the yellow rust reaction using two and three band spectral indices. It was determined that the early-mid growth stage (flowering) is important for the detection and control of diseases, and the mid-late growth stage (grain development) is important for estimating crop losses.

5. Conclusion

Observations were evaluated using multi-correlation and analysis of variance (One-Way ANOVA) technique, and according to the results obtained, it was concluded that visible bands in the early-mid developmental period and Near Infrared Regions in the mid-late period are more decisive in the diagnosis of the disease. Compared to the healthy wheat plant, the spectral reflectance values of the yellow rust-infected wheat plants increased in the visible region during the same growth period, while a decrease was detected in the Near Infrared region. In the early middle period (10.5.1), which is the beginning of flowering (on 25 May, 2019) in Eser, Bayraktar 2000, Kenanbey and Demir 2000 varieties with no disease observed among the bread wheat varieties, low reflectance values were detected in the visible region bands, and an increase has been observed in the reflectance values from the Red region. A decrease in reflection values was determined in the Near Infrared region in the mid-late period (10.5.3) which is the grain setting period (on 06 June, 2019) and the late period (10.5.4) which is the milk production period.

Similar to bread varieties, the beginning of flowering (on 25 May, 2019) in durum varieties were observed in the visible region bands in the early middle period (10.5.1), while low reflectance values were observed. The highest reflectance values were determined, especially in the Near Infrared Region, starting from the Red region in plants without disease. In the advanced stages of development, a decreasing trend in reflectance values was determined in the Near Infrared Region bands.

Acknowledgement

This study was conducted by Metin AYDOĐDU in the master's thesis "Determination of the Seasonal Effects of Different Iron and Zinc Applications on Yellow Rust (*Puccinia striiformis* f. sp. *tritici*) Disease in Winter Wheat Using Multi-Band Data" at Kırşehir Ahi Evran University, Institute of Science, Department of Agricultural Biotechnology (YÖK Thesis No: 671046/Date: 25.05.2021). We would like to thank to Dr. Nilüfer AKCI who works in the Department of Plant Diseases of the Central Research Institute of Agricultural Control for contribution to the preparation and execution of the thesis, to Thesis Monitoring Committee members Prof. Dr. Hikmet GÜNAL (Harran University) and Dr. Nurullah ACİR (Kırşehir Ahi Evran University) for their contributions.

References

- Abburu, S., & Golla, S. B. (2015). Satellite image classification methods and techniques: A review. *International Journal of Computer Applications*, 119(8), 20-24.
- Akan, K. (2019). Sarı pas (*Puccinia striiformis* f. sp. *tritici*) hastalığına dayanıklı makarnalık buğday hatlarının geliştirilmesi. *Türk Tarım ve Doğa Bilimleri Dergisi*, 6(4), 661-670.

- Aktař, H., Karaman, M., Tekdal, S., Kılıc, H., & Kendal, E. (2012, August). Evaluating of yield losses caused by yellow rust pressure in some bread wheat genotypes. In *13th International Cereal Rusts and Powdery Mildews Conference, 2012. Proceedings.* (pp. 16).
- Bravo, C., Moshou, D., West, J., McCartney, A., & Ramon, H. (2003). Early disease detection in wheat fields using spectral reflectance. *Biosystems Engineering*, *84*(2), 137-145.
- Broge, N. H., & Leblanc, E. (2001). Comparing prediction power and stability of broadband and hyperspectral vegetation indices for estimation of green leaf area index and canopy chlorophyll density. *Remote Sensing of Environment*, *76*(2), 156-172.
- Chen, J. M., & Cihlar, J. (1996). Retrieving leaf area index of boreal conifer forests using Landsat TM images. *Remote Sensing of Environment*, *55*(2), 153-162.
- Chen, X. M. (2005). Epidemiology and control of stripe rust [*Puccinia striiformis* f. sp. *tritici*] on wheat. *Canadian Journal of Plant Pathology*, *27*(3), 314-337.
- Delwiche, S. R., & Kim, M. S. (2000, December). Hyperspectral imaging for detection of scab in wheat. In *Biological Quality and Precision Agriculture II, 2000. Proceedings.* (pp. 13-20). SPIE.
- Devadas, R., Lamb, D. W., Simpfendorfer, S., & Backhouse, D. (2009). Evaluating ten spectral vegetation indices for identifying rust infection in individual wheat leaves. *Precision Agriculture*, *10*, 459-470.
- Dusunceli, F., Cetin, L., Albustan, S., & Beniwal, S. P. S. (1996, September). Occurrence and impact of wheat stripe rust (*Puccinia striiformis*) in Turkey in 1994/95 crop season. In *9th European and Mediterranean Cereal Rusts and Powdery Mildews Conference, 1996. Proceedings.* (pp. 309).
- Duveiller, G., Weiss, M., Baret, F., & Defourny, P. (2011). Retrieving wheat Green Area Index during the growing season from optical time series measurements based on neural network radiative transfer inversion. *Remote Sensing of Environment*, *115*(3), 887-896.
- FAO. (2020) *FAOSTAT Statistical Database*. Retrieved from <https://www.fao.org/faostat/en/#home>.
- Feng, W., Shen, W., He, L., Duan, J., Guo, B., Li, Y., Wang, C., & Guo, T. (2016). Improved remote sensing detection of wheat powdery mildew using dual-green vegetation indices. *Precision Agriculture*, *17*, 608-627.
- Filella, I., Serrano, L., Serra, J., & Penuelas, J. (1995). Evaluating wheat nitrogen status with canopy reflectance indices and discriminant analysis. *Crop Science*, *35*(5), 1400-1405.
- Gitelson, A. A., Kaufman, Y. J., & Merzlyak, M. N. (1996). Use of a green channel in remote sensing of global vegetation from EOS-MODIS. *Remote Sensing of Environment*, *58*(3), 289-298.
- Gitelson, A. A., Merzlyak, M. N., & Chivkunova, O. B. (2001). Optical properties and nondestructive estimation of anthocyanin content in plant leaves. *Photochemistry and Photobiology*, *74*(1), 38-45.
- Gitelson, A., & Merzlyak, M. N. (1994). Spectral reflectance changes associated with autumn senescence of *Aesculus hippocastanum* L. and *Acer platanoides* L. leaves. Spectral features and relation to chlorophyll estimation. *Journal of Plant Physiology*, *143*(3), 286-292.
- Goetz, A. F., Vane, G., Solomon, J. E., & Rock, B. N. (1985). Imaging spectrometry for earth remote sensing. *Science*, *228*(4704), 1147-1153.
- Gupta, R. K., Vijayan, D., & Prasad, T. S. (2001). New hyperspectral vegetation characterization parameters. *Advances in Space Research*, *28*(1), 201-206.
- Haboudane, D., Miller, J. R., Pattey, E., Zarco-Tejada, P. J., & Strachan, I. B. (2004). Hyperspectral vegetation indices and novel algorithms for predicting green LAI of crop canopies: Modeling and validation in the context of precision agriculture. *Remote Sensing of Environment*, *90*(3), 337-352.
- Haboudane, D., Miller, J. R., Tremblay, N., Zarco-Tejada, P. J., & Dextraze, L. (2002). Integrated narrow-band vegetation indices for prediction of crop chlorophyll content for application to precision agriculture. *Remote Sensing of Environment*, *81*(2-3), 416-426.
- Hatfield, P. L., & Pinter Jr, P. J. (1993). Remote sensing for crop protection. *Crop Protection*, *12*(6), 403-413.
- Huang, W., Guan, Q., Luo, J., Zhang, J., Zhao, J., Liang, D., Huang, L., & Zhang, D. (2014). New optimized spectral indices for identifying and monitoring winter wheat diseases. *IEEE Journal of Selected Topics in Applied Earth Observations and Remote Sensing*, *7*(6), 2516-2524.
- Huang, W., Lamb, D. W., Niu, Z., Zhang, Y., Liu, L., & Wang, J. (2007). Identification of yellow rust in wheat using in-situ spectral reflectance measurements and airborne hyperspectral imaging. *Precision Agriculture*, *8*, 187-197.
- Kavzoglu, T., & Reis, S. (2008). Performance analysis of maximum likelihood and artificial neural network classifiers for training sets with mixed pixels. *GIScience & Remote Sensing*, *45*(3), 330-342.
- Kim, M. S., Daughtry, C. S. T., Chappelle, E. W., McMurtrey, J. E., & Walthall, C. L. (1994). The use of high spectral resolution bands for estimating absorbed photosynthetically active radiation (A par). In *6th International Symposium on Physical Measurements and Signatures in Remote Sensing, 1994. Proceedings.* (pp. 299-306). CNES.
- Large, E. C. (1954). Growth stages in cereals. Illustration of the Feekes scale. *Plant Pathology*, *3*, 128-129.

- Liu, L., Dong, Y., Huang, W., Du, X., Ren, B., Huang, L., Zheng Q., & Ma, H. (2020). A disease index for efficiently detecting wheat fusarium head blight using Sentinel-2 multispectral imagery. *IEEE Access*, 8, 52181-52191.
- Merton, R., & Huntington, J. (1999, February). Early simulation results of the ARIES-1 satellite sensor for multi-temporal vegetation research derived from AVIRIS. In *Eighth Annual JPL Airborne Earth Science Workshop, 1999. Proceedings.* (pp. 9-11). NASA.
- Merzlyak, M. N., Gitelson, A. A., Chivkunova, O. B., & Rakitin, V. Y. (1999). Non-destructive optical detection of pigment changes during leaf senescence and fruit ripening. *Physiologia Plantarum*, 106(1), 135-141.
- Moshou, D., Bravo, C., Oberti, R., West, J., Bodria, L., McCartney, A., & Ramon, H. (2005). Plant disease detection based on data fusion of hyper-spectral and multi-spectral fluorescence imaging using Kohonen maps. *Real-Time Imaging*, 11(2), 75-83.
- Moshou, D., Bravo, C., West, J., Wahlen, S., McCartney, A., & Ramon, H. (2004). Automatic detection of 'yellow rust' in wheat using reflectance measurements and neural networks. *Computers and Electronics in Agriculture*, 44(3), 173-188.
- Naidu, R. A., Perry, E. M., Pierce, F. J., & Mekuria, T. (2009). The potential of spectral reflectance technique for the detection of Grapevine leafroll-associated virus-3 in two red-berried wine grape cultivars. *Computers and Electronics in Agriculture*, 66(1), 38-45.
- Nicolas, H. (2004). Using remote sensing to determine of the date of a fungicide application on winter wheat. *Crop Protection*, 23(9), 853-863.
- Nilsson, H. (1995). Remote sensing and image analysis in plant pathology. *Annual Review of Phytopathology*, 33(1), 489-528.
- Oppelt, N., & Mauser, W. (2004). Hyperspectral monitoring of physiological parameters of wheat during a vegetation period using AVIS data. *International Journal of Remote Sensing*, 25(1), 145-159.
- Peñuelas, J., Gamon, J. A., Fredeen, A. L., Merino, J., & Field, C. B. (1994). Reflectance indices associated with physiological changes in nitrogen-and water-limited sunflower leaves. *Remote Sensing of Environment*, 48(2), 135-146.
- Peñuelas, J., Pinol, J., Ogaya, R., & Filella, I. (1997). Estimation of plant water concentration by the reflectance water index WI (R900/R970). *International Journal of Remote Sensing*, 18(13), 2869-2875.
- Peterson, R. F., Campbell, A. B., & Hannah, A. E. (1948). A diagrammatic scale for estimating rust intensity on leaves and stems of cereals. *Canadian Journal of Research*, 26(5), 496-500.
- Qin, Z., & Zhang, M. (2005). Detection of rice sheath blight for in-season disease management using multispectral remote sensing. *International Journal of Applied Earth Observation and Geoinformation*, 7(2), 115-128.
- Roelfs, A. P. (1978). Estimated losses caused by rust in small grain cereals in the United States, 1918-76. In A. P. Roelfs (Eds.), *Estimated losses caused by rust in small grain cereals* (pp. 1356-1372). Washington DC: US Department of Agriculture, Agricultural Research Service.
- Roelfs, A. P., Singh, R. P., & Saari, E. E., (1992). *Rust Diseases of Wheat: Concepts and Methods of Disease Management*. Mexico, D.F.: CIMMYT.
- Samborski, D. J. (1985). Wheat leaf rust. In A.P. Roelfs & W.R. Bushnell (Eds.), *Diseases, distribution, epidemiology, and control* (pp. 39-59). Cambridge, Massachusetts: Academic Press.
- Strange, R. N., & Scott, P. R. (2005). Plant disease: a threat to global food security. *Annual Review of Phytopathology*, 43(1), 83-116.
- Thenkabail, P. S., Smith, R. B., & De Pauw, E. (2000). Hyperspectral vegetation indices and their relationships with agricultural crop characteristics. *Remote Sensing of Environment*, 71(2), 158-182.
- Ustuner, M., Sanli, F. B., & Dixon, B. (2015). Application of support vector machines for land use classification using high-resolution rapideye images: A sensitivity analysis. *European Journal of Remote Sensing*, 48(1), 403-422.
- Yu, K., Anderegg, J., Mikaberidze, A., Karisto, P., Mascher, F., McDonald, B. A., Walter, A., & Hund, A. (2018). Hyperspectral canopy sensing of wheat *Septoria tritici* blotch disease. *Frontiers in Plant Science*, 9, 1195. doi: 10.3389/fpls.2018.01195.
- Zadoks, J.C., Chang, T.T. and Konzak, C.F. (1974) A decimal code for the growth stages of cereals. *Weed Research*, 14, 415-21.
- Zarco-Tejada, P. J., Berjón, A., Lopez-Lozano, R., Miller, J. R., Martín, P., Cachorro, V., González, M. R., & De Frutos, A. (2005). Assessing vineyard condition with hyperspectral indices: Leaf and canopy reflectance simulation in a row-structured discontinuous canopy. *Remote Sensing of Environment*, 99(3), 271-287.
- Zhang, J. C., Pu, R. L., Wang, J. H., Huang, W. J., Yuan, L., & Luo, J. H. (2012a). Detecting powdery mildew of winter wheat using leaf level hyperspectral measurements. *Computers and Electronics in Agriculture*, 85, 13-23.
- Zhang, J., Huang, W., Li, J., Yang, G., Luo, J., Gu, X., & Wang, J. (2011). Development, evaluation and application of a spectral knowledge base to detect yellow rust in winter wheat. *Precision Agriculture*, 12, 716-731.
- Zhang, J., Pu, R., Huang, W., Yuan, L., Luo, J., & Wang, J. (2012b). Using in-situ hyperspectral data for detecting and discriminating yellow rust disease from nutrient stresses. *Field Crops Research*, 134, 165-174.

Zhao, C., Huang, M., Huang, W., Liu, L., & Wang, J. (2004). Analysis of winter wheat stripe rust characteristic spectrum and establishing of inversion models. In *IEEE International Geoscience and Remote Sensing Symposium, 2004. Proceedings.* (pp. 4318-4320). IEEE.